

Land cover changes implications in energy flow and water cycle in São Francisco Basin, Brazil, over the past seven decades

Vitor Juste dos Santos¹, Maria Lucia Calijuri², and Leonardo Campos Assis³

¹Federal University of Viçosa

²Universidade Federal de Viçosa

³Universidade de Uberaba

November 22, 2022

Abstract

This research aimed to quantify and qualify alterations in land cover and verify the implications of these modifications for variables related to energy flows and water cycle in São Francisco basin (SFB), located entirely in Brazilian territory, in the second half of the 20th century and beginning of the 21st. For this, statistical analyzes (descriptive, trends, seasonal and correlations) were used to quantify changes in the variables of land cover and energy/water flows, in addition to relating them. As a result, it was found that the SFB lost 65,680 km² of native vegetation (10.4% of basin area) to crops and pastures, reducing water infiltration (-52%) while the rains remained stable (-2%). Water loss increased through evapotranspiration (+5%) and surface runoff (+225%). Such changes in the water cycle have entailed an 11% reduction in São Francisco river long term flow rate (Q_{95}), comparing pre and post-1990s period. In SFB, the activities that required water, such as farming activities, are those that promote hydric loss.

Land cover changes implications in energy flow and water cycle in São Francisco Basin, Brazil, over the past seven decades

V.J. dos Santos¹, M. L. Calijuri¹, L. C. de Assis²

¹ Civil Engineering Department, Federal University of Viçosa, Av. Peter Henry Rolfs, s/n, Campus Universitário, Viçosa-MG, 36570-900, Brazil. E-mails: vjustedossantos@gmail.com and lucia.calijuri@gmail.com.

² Environmental Engineering Department, University of Uberaba - Uniube, Av. Nenê Sabino, 1801, Campus Aeroporto, Uberaba-MG, 38055-500, Brazil. E-mail: leonardo.assis@uniube.br.

Corresponding Author: Vitor Juste dos Santos (vjustedossantos@gmail.com).

Key-Points:

- 65,680 km² of native vegetation loss (10.4% of basin area) to crops and pastures;
- Water inflow by rain kept stable (-2%) and infiltration was reduced (-52%). Water loss increased through evapotranspiration (+5%) and surface runoff (+225%);
- São Francisco river flow rate reduced 11%, comparing pre and post-1990s period. The activities that need water are those that promote hydric loss in the basin.

Abstract:

This research aimed to quantify and qualify alterations in land cover and verify the implications of these modifications for variables related to energy flows and water cycle in São Francisco basin (SFB), located entirely in Brazilian territory, in the second half of the 20th century and beginning of the 21st. For this, statistical analyzes (descriptive, trends, seasonal and correlations) were used to quantify changes in the variables of land cover and energy/water flows, in addition to relating them. As a result, it was found that the SFB lost 65,680 km² of native vegetation (10.4% of basin area) to crops and pastures, reducing water infiltration (-52%) while the rains remained stable (-2%). Water loss increased through evapotranspiration (+5%) and surface runoff (+225%). Such changes in the water cycle have entailed an 11% reduction in São Francisco river long term flow rate (Q_{95}), comparing pre and post-1990s period. In SFB, the activities that required water, such as farming activities, are those that promote hydric loss.

Key-Words:

Correlation; Flow Rate; Rainfall; Trend Analysis; Water Balance; Water Loss

37 **1 Introduction**

38 Investigating Earth's energy and water cycle is essential to understand global climate
39 dynamics and how it impacts and is influenced by human actions (Seyoum & Milewski, 2017;
40 Umair et al., 2019). The terrestrial climate is susceptible to radiation flows, both those of short-
41 wave originating from solar activities and those of long-wave from solar rays' irradiation on the
42 planet's surface (Mokhtari et al., 2018; Yan et al., 2020; Yang et al., 2017).

43 In addition to the intensity of solar activities, the balance of terrestrial radiation will
44 depend on atmosphere composition, land cover, relief, and the amount of surface water present
45 in the upper lithosphere (Jiang et al., 2021; Mokhtari et al., 2018; Yan et al., 2020). It is already
46 known, therefore, that the energy flux on Earth will depend on the interaction between its various
47 spheres (Atmosphere, Lithosphere, Hydrosphere and Biosphere). It is also known that man,
48 nowadays, can influence these different spheres, changing energy and water flows among them,
49 with their actions that change land cover and atmosphere chemical composition (Rodell et al.,
50 2004; Umair et al., 2019).

51 Precipitated water will be distinguished into two main categories (Umair et al., 2019): i)
52 first is the demand for water required by the atmosphere, called potential evapotranspiration,
53 which will convert part of the water present in the lithosphere, hydrosphere and biosphere into
54 real evapotranspiration, not always reaching the total potential demand, as there is dependence
55 on the amount of water present in the environment (Jiang et al., 2021); ii) second is the surface
56 and subsurface runoff, which the balance between these will depend on relief, soils type, land
57 cover, human activities and atmospheric water demand (Ala-aho et al., 2017; Umair et al., 2019).
58 About 67% of the precipitated water across the globe is converted to moisture into the
59 atmosphere by evapotranspiration (Umair et al., 2019).

60 Although the planet has its dynamics in terms of energy and water flows, human beings,
61 mainly after the industrial revolution (Lindsey, 2009), begin to participate in these complex
62 cycles more significantly. Its activities, such as deforestation, irrigation, urbanization, mining,
63 among others, are vectors of changes in terrestrial land cover and atmospheric chemical
64 composition. In turn, they directly influence energy flows, altering the radiation balance and,
65 consequently, the heat flow (sensitive and latent), which in turn will influence and modify the
66 planet's surface temperature and cause changes in water exchanges between surface and
67 atmosphere (Das et al., 2018; Umair et al., 2019).

68 To understand these complex interactions between the terrestrial spheres, initiatives
69 emerged, such as the Land Data Assimilation System (LDAS) (<https://ldas.gsfc.nasa.gov/>). This
70 is developed by the Hydrological Sciences Laboratory of the Goddard Space Flight Center
71 belonging to the National Aeronautics and Space Administration (NASA). With numerical
72 models use, physical processes inherent in the interactions between Earth's surface and
73 atmosphere are modeled from data collected in the field and by orbital images.

74 From the results, several LDAS projects were developed, which are the Global Land Data
75 Assimilation System (GLDAS), the North American Land Data Assimilation System (NLDAS),
76 the National Climate Assessment - Land Data Assimilation System (NCA-LDAS) and the
77 Famine Early Warning System Network (FEWS NET) Land Data Assimilation System
78 (FLDAS). All of these projects have in common the study and understanding of energy and
79 water terrestrial fluxes, but with different areas and technical specifications with the database
80 used, according to the regional reality.

81 The use of information generated by models like as LDAS program helps in water
82 resources management, as it is possible to carry out monitoring of drought events, numerical
83 studies of the weather forecast and scientific investigations of water and energy flows (Rodell et
84 al., 2004). Without the application of such models, it would be even more difficult and costly to
85 monitor energy and humidity dynamics with frequent periodicity and adequate geographic scale
86 (Mokhtari et al., 2018; Yang et al., 2017).

87 Several studies have been carried out based on data generated by LDAS, as the impacts
88 caused by changes in land use and land cover on surface runoff and energy flows, under different
89 climatic conditions, in East Asia (Umair et al., 2019), or to measure water consumption in
90 irrigating crops in agricultural areas in China (Yin et al., 2020). In addition to these, others used
91 data from LDAS to investigate what are the climatic forces associated with occurrences of
92 droughts and wet periods across the planet (Yuan et al., 2019). There are several other examples
93 of studies, which can be found on LDAS website.

94 In this context, the objective of this research is to identify and measure changes in the
95 energy flow and water cycle in São Francisco Basin (SFB) in the second half of the 20th century
96 and the first two decades of the 21st, and verifying the implications of land cover modifications,
97 caused by human activities in the last four decades, in changes caused in these cycles' dynamics.
98 Although studies have already been carried out for the basin in this sense, there are still certain

99 gaps concerning changes in the inlet and outlet of water and energy, alterations that have been
100 influenced by human activities.

101 The most recent SFB studies dealing with the water cycle focus on issues related to water
102 availability and demand. Sun et al. (2016) identified a loss rate of 3.3 km³ of water per year over
103 13 years of assessment (between 2002 and 2015), caused mainly by the drought that started in
104 2012 and ended in 2017, which resulted in a loss rate of 27.63 km³ between 2012 and 2015. In
105 this study, data on precipitation and stored water present on the earth's surface were used, and the
106 influence of the *El Niño* phenomenon on drought period occurrence.

107 In another research, by Koch et al. (2015), water availability and demand were assessed
108 under two scenarios: i) a regionalized world with slow economic development, high population
109 growth and little awareness of environmental problems; ii) a globalized world with low
110 population growth, high growth in Gross National Product (GNP) and environmental
111 sustainability, also adding climate change scenarios to both. As a result, they found that between
112 2021 and 2050 the basin will be wetter, with more intense rainy and dry periods, and increased
113 water availability for irrigation and a drop in electricity generation.

114 In addition to these, some other studies highlight that hydroelectric energy production
115 may cease in this first half of the 21st century in drought periods (de Jong et al., 2018). Also the
116 prices of agricultural products generated in SFB will be affected, which will depend on climate
117 change, the production location, variety of products and production technology (Torres et al.,
118 2012). It is as well estimated that economic values of water for use in irrigation tend to increase
119 in the coming decades (Alcoforado de Moraes et al., 2018).

120 Although they are important researches, none of them deal with implications that changes
121 in land cover, having as vectors the anthropic activities, cause in the energy flows and water
122 cycle in SFB, a theme that will be the focus of this research.

123 **2 Materials and Methods**

124 The stages of this research were organized as follows (Figure 1): i) study area
125 determination; ii) definition of variables to be studied; iii) statistical analysis of the variables
126 defined in study area over the available historical series; iv) spatiotemporal analysis of the
127 studied variables; v) evaluation of impacts on the water availability in São Francisco River
128 caused by changes in the studied variables.

129

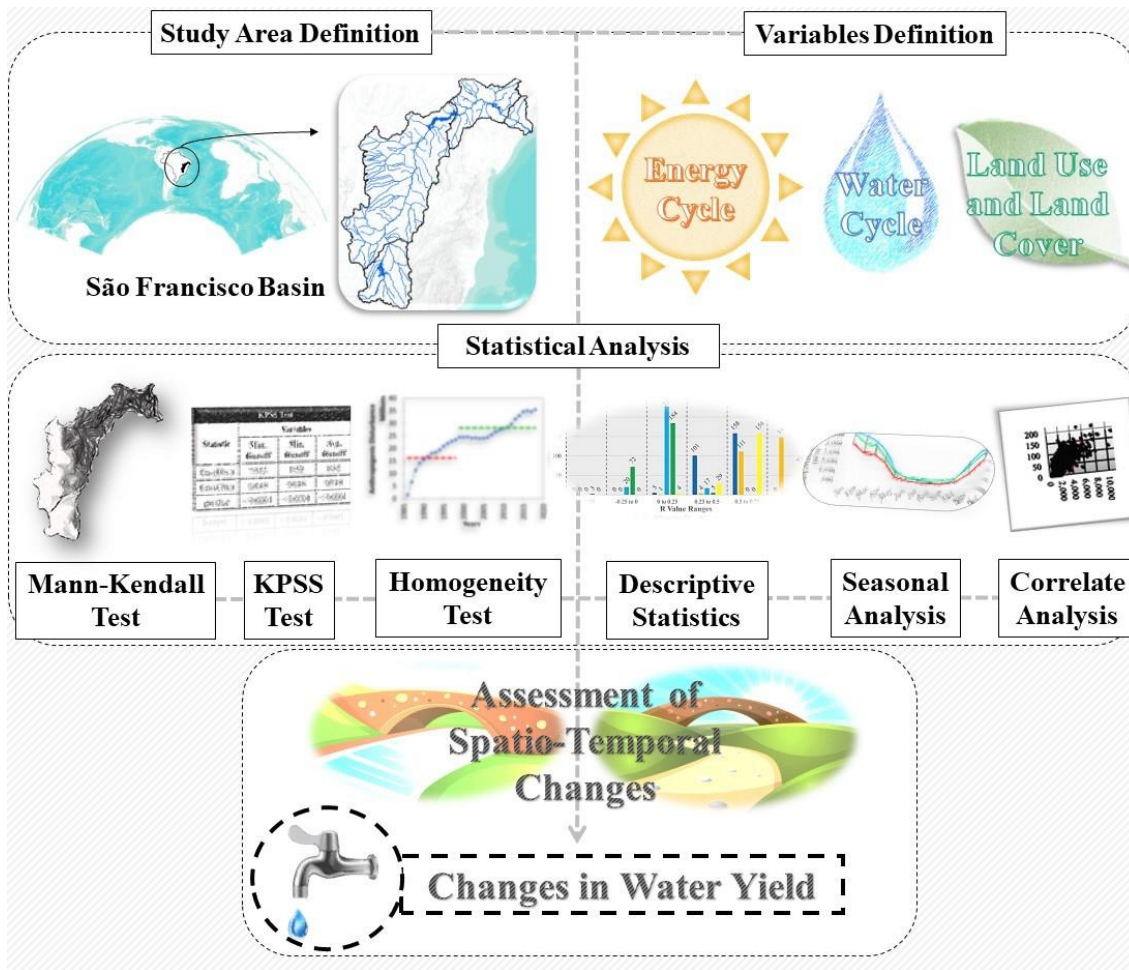


Figure 1 – Methodological flowchart

130
131

132 **2.1 Study Area**

133 The São Francisco Basin (SFB) (Figure 2) is located in the Northeast and North of the
 134 Southeast of Brazil, with an area of 630,000 km² and with its main river running 3,200 km from
 135 the source, in the State of Minas Gerais, at its mouth, on the border of the States of Alagoas and
 136 Sergipe, flowing into South Atlantic Ocean (Bezerra et al., 2019; de Jong et al., 2018). It is
 137 between the latitudes of 21° and 7° South, with climatic characteristics, according to the revised
 138 classification of Thornthwaite (Feddema, 2005), ranging from humid and wet sub-humid types
 139 between latitudes 21° and 10° South (29% of basin area), until dry sub-humid, semi-arid and arid
 140 types between latitudes 17° and 7° South (71%).

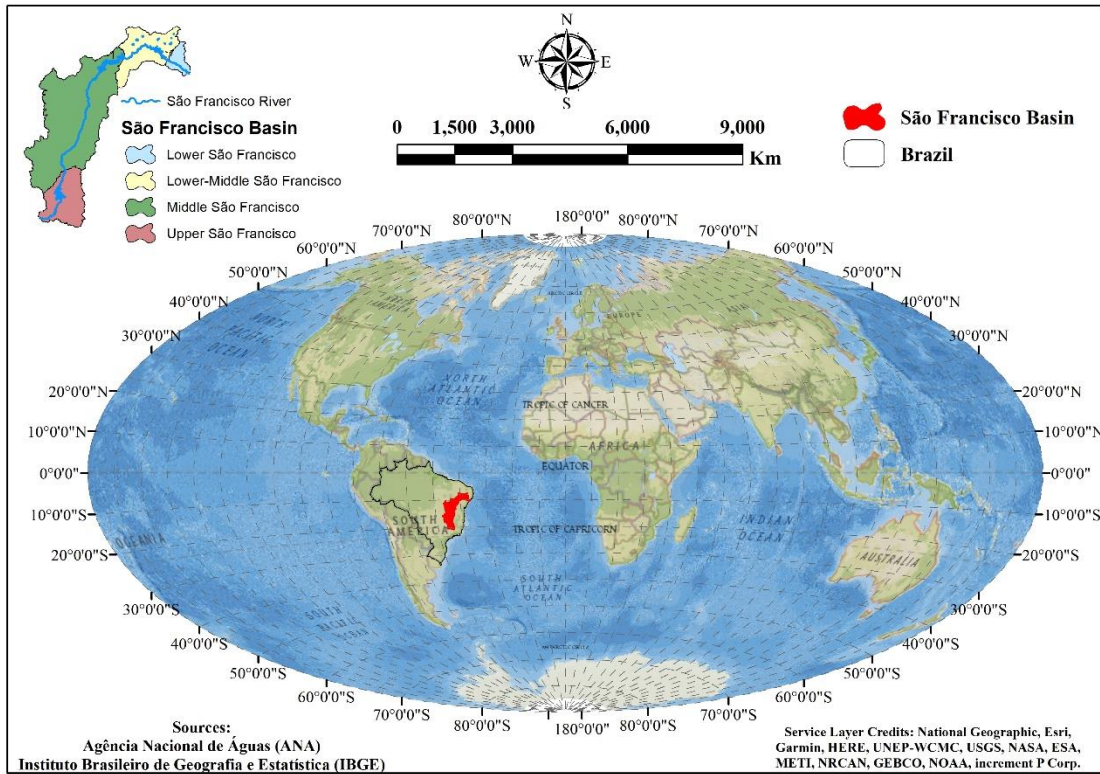


Figure 2 – Study area location

141
142
143

144 In humid and wet sub-humid areas, south and southwest of basin, temperatures reach an
145 average of 20°C (Torres et al., 2012), with potential evapotranspiration ranging from 1,241 to
146 4,344 mm/year, with an average of 2,300 mm/year (Beaudoin & Rodell, 2019), and rains
147 precipitate an average of 1,500 to 2,000 mm/year (Koch et al., 2015; Sun et al., 2016). In dry
148 sub-humid, semi-arid and arid areas, north and northeast of basin, temperatures reach an average
149 of 26.5°C (Torres et al., 2012), with potential evapotranspiration ranging from 1,533 to 5,110
150 mm/year, with an average of 2,884 mm/year (Beaudoin & Rodell, 2019), and rainfall
151 precipitates an average of 350 mm/year (Koch et al., 2015; Sun et al., 2016).

152 Precipitation in humid and wet sub-humid areas is mainly associated with the South
153 Atlantic Convergence Zone (SACZ) that operates in the southeastern region of Brazil and
154 southwestern Bahia during the summer (between October and March) (Torres et al., 2012). In the
155 dry sub-humid, semi-arid and arid areas, rains are concentrated during the months of March and
156 April, caused mainly by action of the Intertropical Convergence Zone (ITCZ), which acts more
157 intensely in this period due to weakening of the inter-hemispheric south gradient of sea surface
158 temperature, which allows ITCZ to reach regions further south. In the rest of the year, there is a

159 strong presence of a high-level cyclone over the Amazon, which inhibits rains formations in the
160 region and favors dry weather conditions, which is often enhanced by strong *El Niño* events.

161 The humid and wet sub-humid areas cover almost all the sub-regions of Upper São
162 Francisco and western part of the Middle. The main river has its contribution mainly from these
163 areas, which were responsible for 93%, between 1951 and 1999, of total permanence flow curves
164 (Q_{95}). That is, approximately 43% of basin was responsible for maintaining flow rate that flowed
165 through the riverbed 95% of the time. The other 57%, corresponding to the sub-regions of Low,
166 Lower-Middle, and eastern part of the Middle São Francisco, which are mostly covered by dry
167 sub-humid, semi-arid and arid areas, contributed with remaining 7% of Q_{95} (Pereira et al., 2007;
168 Pruski et al., 2004). This showing the importance of the areas closest to its source for
169 maintenance of main river.

170 São Francisco has an average flow rate of 2,850 m³/s, ranging from 1,077 to 5,290 m³/s
171 (Bezerra et al., 2019), with a permanence flow curve (Q_{95}) of 800.4 m³/s (Pereira et al., 2007;
172 Pruski et al., 2004). It comes from 70% of the surface waters of entire Northeast region of Brazil
173 (Torres et al., 2012), which has a population of over 53 million people, approximately a quarter
174 of the Brazilian population. Besides, hydroelectric system of this river normally meets 70% of
175 the demand for electricity in Northeast region (de Jong et al., 2018).

176 Added to these hydrological conditions, the basin has vegetations of Cerrado types
177 (Savannah Formation) with a great diversity of tree vegetations (Forest Formation) in Upper and
178 western sub-region of Middle São Francisco, as well as the vegetation of Caatinga biome, which
179 is widely spaced and smaller, associated with drier and hotter climate in Low, Lower-Middle and
180 east of Middle São Francisco (Creech et al., 2015).

181 Land use is predominantly agricultural, with crops (46%) and pastures (41%) dominating
182 the land cover in basin. Aside from, there are remnants of large and medium-sized tree
183 vegetation, urban areas, mining, among others. The main agricultural production is soy, with
184 other major crops such as corn, wheat and cotton, in addition to important fruit centers (Juazeiro
185 and Petrolina) (R. C. Correia et al., 2001) and family farming throughout the basin. Vegetations,
186 crops and pastures are on soils of latosol (41% of the basin), podzols (11%), sandy soils (10%)
187 and cambisols (7%) (Alcoforado de Moraes et al., 2018; Creech et al., 2015; Torres et al., 2012).

188 Covering approximately 7.5% of the Brazilian territory, SFB has a population of over 17
189 million people (8% of Brazilian population), 21% of which are considered poor by the country's

190 standards (Sun et al., 2016). Due to population growth and the demand for food, water, jobs and
191 services, the municipalities in basin have had satisfactory socio-economic development in recent
192 decades, but at the cost of natural resources, mainly native vegetation, soil and water, relative
193 with deforestation problems, desertification, water scarcity, pollution and water bodies silting up
194 (Creech et al., 2015; de Jong et al., 2018; Koch et al., 2015).

195 From the above, it is clear that SFB has significant physical-natural and socioeconomic
196 diversity, which are dynamic in space and time. Due to these factors, the basin was defined as a
197 study area precisely because of its dynamics and diversity related to environmental and human
198 aspects, which interfere with each other. The choice focused on dynamics pertinent to energy and
199 water cycles, which are affected by the basin's socio-economic activities, but also affect them.
200 The option for the area is also linked to the fact that the basin has one of the main rivers in
201 Brazil, entirely within the national territory, which passes through the driest region and one of
202 the poorest in the country. The river has great national importance due to its strong potential for
203 economic use, mainly linked to agricultural activities, irrigation, public supply, navigation and
204 generation of electric energy, but has been under strong pressure exactly by exploration of these
205 same activities.

206 **2.2 Variables Definition**

207 The variables defined in this research were those related to the energy flow and water
208 cycle in SFB, as well as those that can interfere in these cycles, referring to land use and land
209 cover, in addition to the minimum, average and maximum flows rate of São Francisco river
210 (Table 1). The GLDAS database units have been converted, as suggested on Land Data
211 Assimilation System website (<https://ldas.gsfc.nasa.gov/faq/ldas>), for better comparison between
212 variables.

213 The Global Land Data Assimilation System (GLDAS) is a program from the National
214 Aeronautics and Space Administration (NASA) in which observational data from orbital images
215 and information collected in the field are used to model the dynamics of terrestrial phenomena
216 linked to energy flow and the water cycle of the planet Earth. Produces results almost in real-
217 time, with resolutions that vary between 2.5° and 1 km, with historical series between 1948 until
218 today with periodic update (Beaudoing & Rodell, 2019; Rodell et al., 2004).

219 The data used in GLDAS contains relief information, soil types, vegetation and
220 atmospheric variables such as rain and radiation flows. Data assimilation techniques are

221 employed to incorporate hydrological products based on satellite sensor imaging that include
 222 snow cover and water equivalent, soil moisture, surface temperature and leaf area indexes
 223 (Beaudoin & Rodell, 2019; Rodell et al., 2004).

224 **Table 1** - Database used

GLDAS (1948 - 2019) [https://ldas.gsfc.nasa.gov/gldas]		Dataset	Converted
		Units	Units
Swnet	Shortwave Radiation Flow	W/m ²	W/m ²
Lwnet	Long Wave Radiation Flow	W/m ²	W/m ²
Qh	Sensitive Heat Flow	W/m ²	W/m ²
Qle	Latent Heat Flow	W/m ²	W/m ²
Rainf	Rainfall Rate	Kg/m ² /s	mm
AvgSurfT	Average Surface Temperature	K	°C
PotEvap	Potential Evapotranspiration	W/m ²	mm
Evap	Real Evapotranspiration	Kg/m ² /s	mm
Tveg	Vegetation Transpiration	W/m ²	mm
Ecanop	Direct Evaporation of Plants Canopy	W/m ²	mm
Esoil	Direct Evaporation of Bare Soil	W/m ²	mm
Canint	Moisture in Plants Canopy	Kg/m ²	mm
RootMoist	Root Zone Soil Moisture	Kg/m ²	mm
Qs	Surface Runoff	Kg/m ² /3h	mm
Qsb	Subsurface Runoff	Kg/m ² /3h	mm
MapBiomias (1985 - 2018) [https://mapbiomas.org/]		Dataset	Converted
		Units	Units
LULC	Lan Use and Land Cover	-	-
MEaSURES [https://lpdaac.usgs.gov/data/get-started-data/collection-overview/measures/]		Dataset	Converted
		Units	Units
VCF	Tree Cover	Percent Tree Cover (1982 - 2014)	%
	Non-Tree Cover	Percent Non-Tree Cover (1982 - 2014)	%
	Bare Ground	Percent Bare Ground (1982 - 2014)	%
VIP	NDVI	Normalized Difference Vegetation Index (1981 - 2019)	-
ANA (1928 - 2019) [http://www.snirh.gov.br/hidroweb/]		Dataset	Converted
		Units	Units
Flow Rate	Minimum, Average and Maximum Flows Rate	m ³ /s	m ³ /s

225
 226 The Annual Mapping of Land Use and Land Cover in Brazil (MapBiomias) (Souza et al.,
 227 2020) is a collaborative network with specialists in Brazilian biomes, land uses, remote sensing,
 228 geographic information systems and computer science, which uses cloud processing and
 229 automatic classifiers (Random Forest) developed and operated from Google Earth Engine
 230 platform. Since its foundation (2015) it has been generating an annual historical series of land
 231 use and land cover maps for the whole of Brazil (1985 to 2018 - Collection 4.1), with a spatial
 232 resolution of 30 meters using the series of images from Landsat sensors.

233 The program Making Earth System Data Records for Use in Research Environments
234 (MEaSURES), from NASA's Land Processes Distributed Active Archive Center (LP DACC), is
235 dedicated to the advancement of remote sensing and the scientific use of measurements from
236 satellite sensors to expand the understanding of terrestrial system, with production and recording
237 of consistent, high quality and long-term data. Among several databases, those used in this
238 research were the Vegetation Continuous Fields (VCF) (Hansen & Song, 2018) and the
239 Vegetation Index and Phenology (VIP) (Didan & Barreto, 2016). The first is a collection that
240 provides global vegetation information from the Advanced Very High-Resolution Radiometer
241 (AVHRR) long-term records between 1982 and 2014, annually, with a spatial resolution of 5,600
242 m containing information on the percentage of tree vegetation cover, non-tree vegetation cover
243 and bare ground. The second is another collection containing a monthly historical series from
244 1981 to 2019, of vegetation and landscape phenology indexes, based on data from the Moderate-
245 Resolution Imaging Spectroradiometer (MODIS), AVHRR and *Satellite Pour l'Observation de*
246 *la Terre* (SPOT), also with a spatial resolution of 5,600 m.

247 The Hidroweb Portal (<http://www.snirh.gov.br/hidroweb/>) is a Brazilian tool that is part
248 of the National Water Resources Information System (SNIRH, acronym in Portuguese) and
249 offers access to database that contains all information collected by the National
250 Hydrometeorological Network (RHN, acronym in Portuguese), which gathers data on flows rate,
251 river height, rainfall, climatology, sediment and water quality. The data used come from
252 conventional fluviometric stations with codes 45298000 (14.3° S and 43.76° W) and 49705000
253 (10.21 S and 38.82 W), with historical series of daily and monthly frequencies between 1928-
254 2019 and 1959-2019, respectively. The use of these two stations is better detailed in item 3.1, as
255 the choice of both was defined based on some results of this research.

256 **2.3 Statistical Analysis**

257 The statistical procedures were broken down into three stages: i) first performed on
258 variables related to energy flow and water cycle; ii) later on variables related to land use and land
259 cover; iii) and, finally, in the variables related to São Francisco river flow rate and its
260 correlations with the analysis of the previous data.

2.3.1 Statistical analysis on variables related to energy and water cycles

First, the Mann-Kendall test (MK tau) was performed on variables related to energy flow and water cycle, from GLDAS database, monthly, between January 1948 and December 2019.

This first analysis aimed to verify the spatiotemporal behavior of the variables and to search for different trend patterns throughout SFB in the mappings made by the test, pixel by pixel, using the Series Trend tool of the Earth Trend Modeler module available by Idrisi Selva 17.0 software (Eastman, 2016). With the identification of patterns, it was decided to divide the study area into two parts (P1 and P2). This decision is explained in results.

MK tau is a non-parametric trend indicator that measures the degree to which a trend is increasing or decreasing consistently. It was first proposed by Mann (1945) and later studied by Kendall (1975), then enhanced by Hirsch et al. (1982) and Hirsch & Slack (1984), which made it possible to take seasonality into account. It has a range of -1 to +1. A value of +1 indicates a trend that continually increases and never decreases. The opposite is true when it has a value of -1. The zero value indicates that there is no consistent trend. All combinations of pair values over time are evaluated at each pixel and a count is made of the number that is increasing or decreasing over time. It is simply the relative frequency of increases minus the relative frequency of decreases (Eastman, 2016).

With P1 and P2 discriminated, descriptive statistics were made to verify variations of the average values of each variable in both areas, checking if in general there was an increase, stability or decrease in each one of them. Stationarity (KPSS) and homogeneity (Pettitt and Buishand) tests were also performed.

The stationarity test used was the KPSS (Kwiatkowski et al., 1992), which allows to check whether a series is stationary or not. The test result varies from zero to ∞ (Eta Observed Value), in which the higher the critical value (Eta Critical Value), greater the tendency for the series not to be stationary, and the opposite being also true, that is, as closer to zero and below the critical value, greater the tendency to stationarity.

The homogeneity tests used were those by Buishand (1982) and Pettitt (1979), that check if a series is homogeneous over time, or if there is a moment when a change or break in that homogeneity occurs. Such tests were selected based on different sensitivities they present for identification at the change time and because they are widely used to test homogeneity in

291 environmental data series (Bickici Arikan & Kahya, 2019; Rougé et al., 2013; Serinaldi et al.,
292 2018; Serinaldi & Kilsby, 2015; Yozgatligil & Yazici, 2016).

293 **2.3.2 Statistical analysis on variables related to LULC and MEaSURES**

294 To measure changes in land use and land cover in SFB, the Change Analysis tool of Land
295 Change Modeler module, from Idrisi Selva 17.0 software, was used (Eastman, 2016). In this tool,
296 it was possible to verify the main changes between the years 1985 and 2018.

297 In addition to measuring changes in land use and land cover using MapBiomas data, the
298 MEaSURES database was also used, which contains data on the percentage of tree cover, non-
299 tree cover and bare ground (VCF) between 1982 and 2014, and NDVI (VIP) between 1981 and
300 2019, respectively (Didan & Barreto, 2016; Hansen & Song, 2018).

301 For MapBiomas land use and land cover data, from the measurements generated in Land
302 Change Modeler module, all classes related to human actions (Farming, Mining, Planted Forest
303 and Urban Areas) were grouped into a single class called Anthropogenic Disorders. In this,
304 Mann-Kendall and homogeneity tests (Pettitt and Buishand) were performed.

305 In the MEaSURES data, Mann-Kendall test was used to identify differences
306 spatiotemporal trends in the SFB with Series Trend tool of Earth Trend Modeler module from
307 Idrisi Selva 17.0 software aid (Eastman, 2016).

308 **2.3.3 Statistical analysis on variables related to São Francisco river flow rate**

309 The data series on the minimum, average and maximum flows rate of São Francisco river
310 was analysed in two river stations, one located in P1 (code 45298000) and another in P2 (code
311 49705000).

312 Mann-Kendall, stationarity and homogeneity tests were also applied. After the application
313 of this tests and results obtained, these were compared to the results of tests related to the
314 variables of previous topics. This was performed to verify possible implications of changes in
315 land cover, in energy flows and, consequently, in water cycle basin, and the impacts of these
316 processes on flow rate dynamics of São Francisco river at P1 and P2.

317 To reinforce possible influences of changes in land cover in water cycle basin, correlation
318 analyzes between NDVI and variations related to water cycle were performed, with the aid of
319 Correlate module of Idrisi Selva 17.0 software (Eastman, 2016). The main application of the
320 module is to identify areas that correlate with a specific temporal pattern of interest, calculating

321 the correlation coefficient R between one or more predictors (independent) with a time series of
322 images (dependent) for each pixel. In addition, such analyzes were also performed between
323 historical series of average flows rate in P1 and P2 with rainfall, surface and subsurface runoff
324 data, using Pearson's correlation (Barber et al., 2020).

325 **4 Results and Discussion**

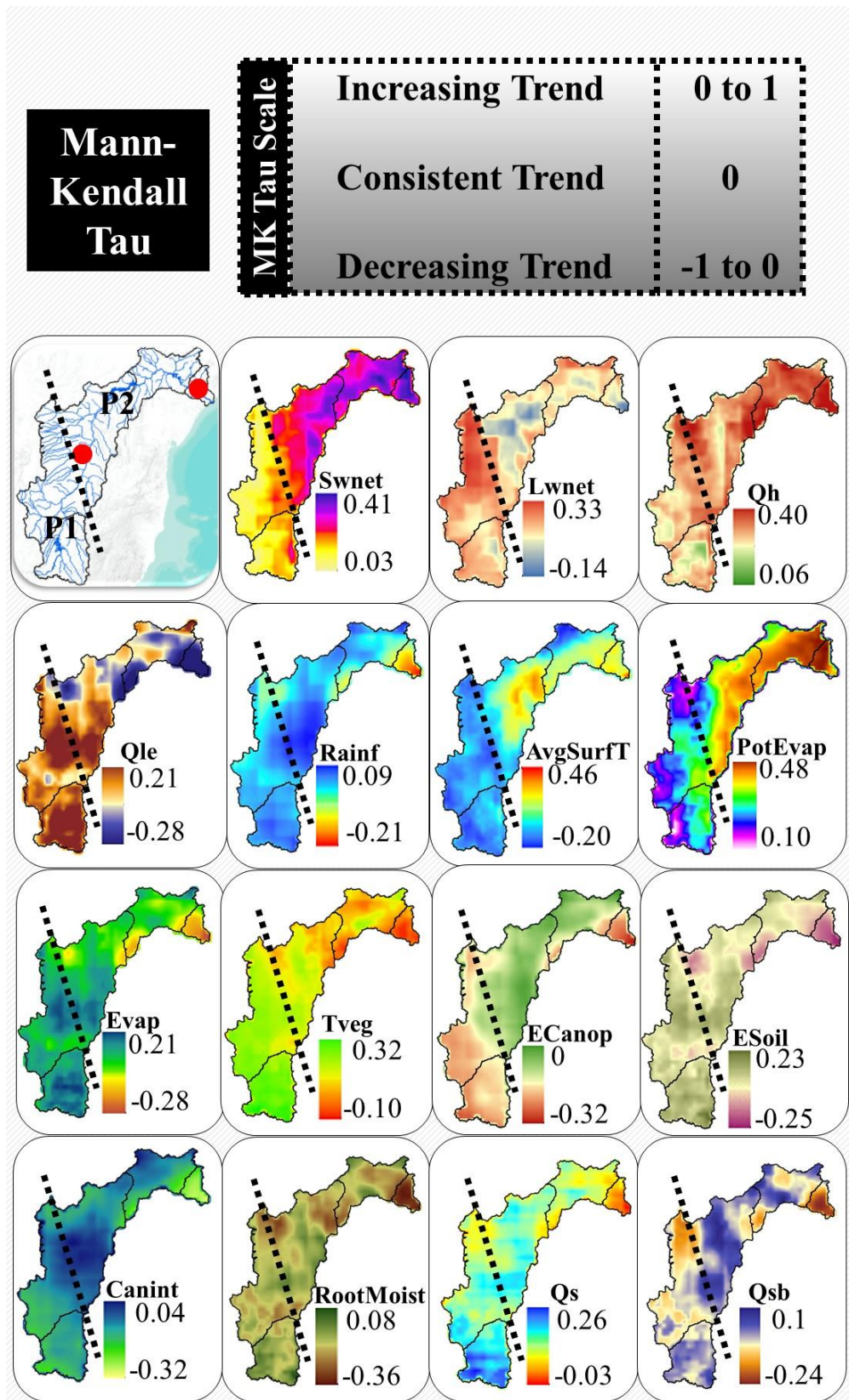
326 This topic is divided into three subtopics, which are: 1) results related to spatiotemporal
327 analysis of energy flow and water cycle variables; 2) results related to spatiotemporal analyzes of
328 land use and land cover and; 3) results and discussion referring to consequences on the dynamics
329 of São Francisco river flow rate resulting from changes in the variables evaluated in the two
330 previous subtopics.

331 **4.1 Spatiotemporal analysis of energy flow and water cycle variables**

332 Mann-Kendall tests carried out for energy flow variables showed that there were different
333 intensities in trends, positive and negative, of radiation flows (short and long waves) and heat
334 (sensitive and latent), in specific areas in SFB between January 1948 and December 2019
335 (Figure 3).

336 Due to this distinctions, the basin was segmented into two parts, P1 and P2 (Figure 3).
337 Such segmentation was based on trends of radiation flows (short and long waves) (Tables 2 and
338 3), which will influence the dynamics of other variables, such as heat flows (sensitive and latent),
339 evapotranspiration and presence of moisture in the canopies and plants root zones. These results
340 also guided the choice for used fluviometric stations locations, aiming to relate the changes in
341 trends of the variables evaluated in GLDAS database with flow rate dynamics. The definition of
342 the fluviometric stations followed two conditions: i) close to the place further downstream from
343 P1 and P2, seeking to cover the entire contribution basin and; ii) with sufficient historical series
344 to satisfactorily cover the period of GLDAS and MEaSURES data.

345 In P1, the predominant trend was from stability to a slight increase in short-wave
346 radiation flow, from 188 to 198 W/m^2 . Regarding long-wave radiation flow, the predominant
347 trend was a slight to moderate increase, from -70 to -64 W/m^2 . Sensitive heat flow also had a
348 predominant tendency to grow from light to moderate, from 49 to 63 W/m^2 . Regarding the latent
349 heat flow, there was a predominantly stable tendency for light growth, from 66 to 71 W/m^2 .



350
351
352

Figure 3 - Trends in variables referring to energy flow and water cycle in SFB between January 1948 and December 2019. The red dots are the fluviometric stations locations with codes 45298000 (P1) and 49705000 (P2).

353 **Table 2** - Trend (MK) range values and significance (p) analyze for energy flow variables in P1.

Variable	MK Tau	Area (%)	p-value	Area (%)
Swnet	0.03 to 0.18	95	0	89
	0.18 to 0.41	5	> 0	11
Lwnet	0 to 0.1	10	0	98
	0.1 to 0.33	90	> 0	2
Qh	0.06 to 0.1	2	0	100
	0.1 to 0.4	98	> 0	0
Qle	-0.04 to 0.1	54	0	79
	0.1 to 0.21	46	> 0	21

354

355 **Table 3** - Trend (MK) range values and significance (p) analyze for energy flow variables in P2.

Variable	MK Tau	Area (%)	p-value	Area (%)
Swnet	0.13 to 0.18	9	0	100
	0.18 to 0.41	91	> 0	0
Lwnet	-0.14 to 0.1	42	0	79
	0.1 to 0.33	58	> 0	21
Qh	0.14 to 0.18	4	0	100
	0.18 to 0.4	96	> 0	0
Qle	-0.28 to 0.1	81	0	54
	0.1 to 0.21	19	> 0	46

356

357 In P2, the predominant trend was for a slight to moderate increase in short-wave radiation
 358 flow, from 193 to 216 W/m². Regarding long-wave radiation flow, the predominant trend was
 359 stability, ranging from -76 to -73 W/m². The predominant trend of sensitive heat flow was
 360 moderate growth, from 65 to 91 W/m². Regarding the latent heat flow, there was a predominantly
 361 stability trend, from 51 to 53 W/m².

362 Even though there are specific cases of mild negative trends, in general, variables related
 363 to radiation and heat flows have positive trends in SFB, in both areas (P1 and P2) (Table 4).

364 **Table 4** – Absolute and relative variations of SFB radiation and heat flow.

Variable	Average Variation - P1		Average Variation - P2	
	Absolute	Relative	Absolute	Relative
Swnet	+ 10 W/m ²	+ 5%	+ 23 W/m ²	+ 12%
Lwnet	+ 6 W/m ²	+ 9%	+ 3 W/m ²	+ 4%
Qh	+ 14 W/m ²	+ 29%	+ 26 W/m ²	+ 40%
Qle	+ 5 W/m ²	+ 12%	+ 2 W/m ²	+ 4%

365

366 This fact contributes to positive trends of potential evapotranspiration throughout the
 367 basin, notably in P2, influenced by significant positive flow of short-wave radiation and specific
 368 heat. Even though the potential evapotranspiration has increased considerably, the real
 369 evapotranspiration, although it has grown, has not followed it (Table 5).

370

371 **Table 5** – Absolute and relative average variations of potential and real evapotranspiration in SFB.

Variable	Average Variation - P1		Average Variation - P2	
	Absolute	Relative	Absolute	Relative
PotEvap	+ 467 mm/year	+ 23%	+ 1072 mm/year	+ 45%
Evap	+ 66 mm/year	+ 8%	+ 31 mm/year	+ 5%

372
373 In P1, the average potential evapotranspiration increased from 2,043 to 2,510 mm/year,
374 while average real evapotranspiration increased from 820 to 883 mm/year. In P2, the average
375 potential evapotranspiration increased from 2,359 to 3,431 mm/year, while average real
376 evapotranspiration increased from 631 to 662 mm/year. This is shown in the trend analysis (MK)
377 results, where for potential evapotranspiration, they were 0.175 and 0.309, P1 and P2
378 respectively. As for the real evapotranspiration, they were 0.04 and zero, P1 and P2 respectively.

379 While there was an increase in potential and real evapotranspiration, pluviometric indexes
380 remained stable (Table 6).

381 **Table 6** – Absolute and relative changes in average rainfall indexes in SFB.

Variable	Average Variation - P1		Average Variation - P2	
	Absolute	Relative	Absolute	Relative
Rainf	- 63 mm/year	- 5%	0 mm/year	0%

382
383 In P1 the average rainfall decreased from 1.324 to 1.261 mm/year, and in P2 there was
384 no variation in the average, remaining at 694 mm/year. The Mann-Kendall analysis confirms
385 such variations, in P1 with a result equal to zero and in P2 equal to 0.005, that is, a tendency to
386 stability.

387 If on average the rainfall rates were stable, which led to an increase in real
388 evapotranspiration in P1 and P2, even if not following the potential evapotranspiration, it was the
389 increase in vegetation transpiration (Table 7), which increased in P1 from 265 to 441 mm/year,
390 and in P2 from 290 to 366 mm/year.

391 **Table 7** – Absolute and relative variations in transpiration/evaporation from different sources in SFB.

Variable	Average Variation - P1		Average Variation - P2	
	Absolute	Relative	Absolute	Relative
Tveg	+ 176 mm/year	+ 66%	+ 76 mm/year	+ 26%
Ecanop	- 127 mm/year	- 37%	- 63 mm/year	- 28%
Esoil	+ 13 mm/year	+ 6%	0 mm/year	0%

392
393 This increase in transpiration was accompanied by a tendency towards stability with a
394 small increase in water evaporation directly from bare soil and a reduction in the plants' canopies
395 evaporation. In P1, there was a tendency for a small increase in bare soil direct evaporation, from

396 227 to 240 mm/year, and a tendency for a decrease in plant' canopy direct evaporation, from 341
 397 to 214 mm/year. In P2, there was a tendency to stability in bare soil direct evaporation,
 398 remaining at 139 mm/year, and again a tendency to decrease in plant' canopy direct evaporation,
 399 from 227 to 164 mm/year.

400 The increase in evapotranspiration was accompanied by a reduction in the presence of
 401 water accumulated in plants' canopies and a decrease in soil moisture in the root zone (Table 8).
 402 In P1, there was a water dip in plants' canopies from 0.19 to 0.12 mm, and a decrease in soil
 403 moisture in root zone from 244 to 228 mm. In P2, there was a water dip in plants' canopies from
 404 0.11 to 0.07 mm, and a decrease in soil moisture in root zone from 210 to 179 mm.

405 **Table 8** – Absolute and relative average variations in the presence of moisture in canopies and root zone of plants in
 406 SFB.

Variable	Average Variation - P1		Average Variation - P2	
	Absolute	Relative	Absolute	Relative
CanopInt	- 0.07 mm	- 37%	- 0.04 mm	- 36%
RootMoinst	- 16 mm	- 7%	- 31 mm	- 15%

407

408 Additionally, there was an increase in surface runoff and a decrease in subsurface runoff
 409 (Table 9). In P1, there was an increase in surface runoff from 16 to 80 mm/year and a decrease in
 410 subsurface runoff from 445.6 to 283.2 mm/year. In P2, there was an increase in surface runoff
 411 from 0.8 to 38.4 mm/year, and a drop in subsurface runoff from 126.4 to 38.4 mm/year.

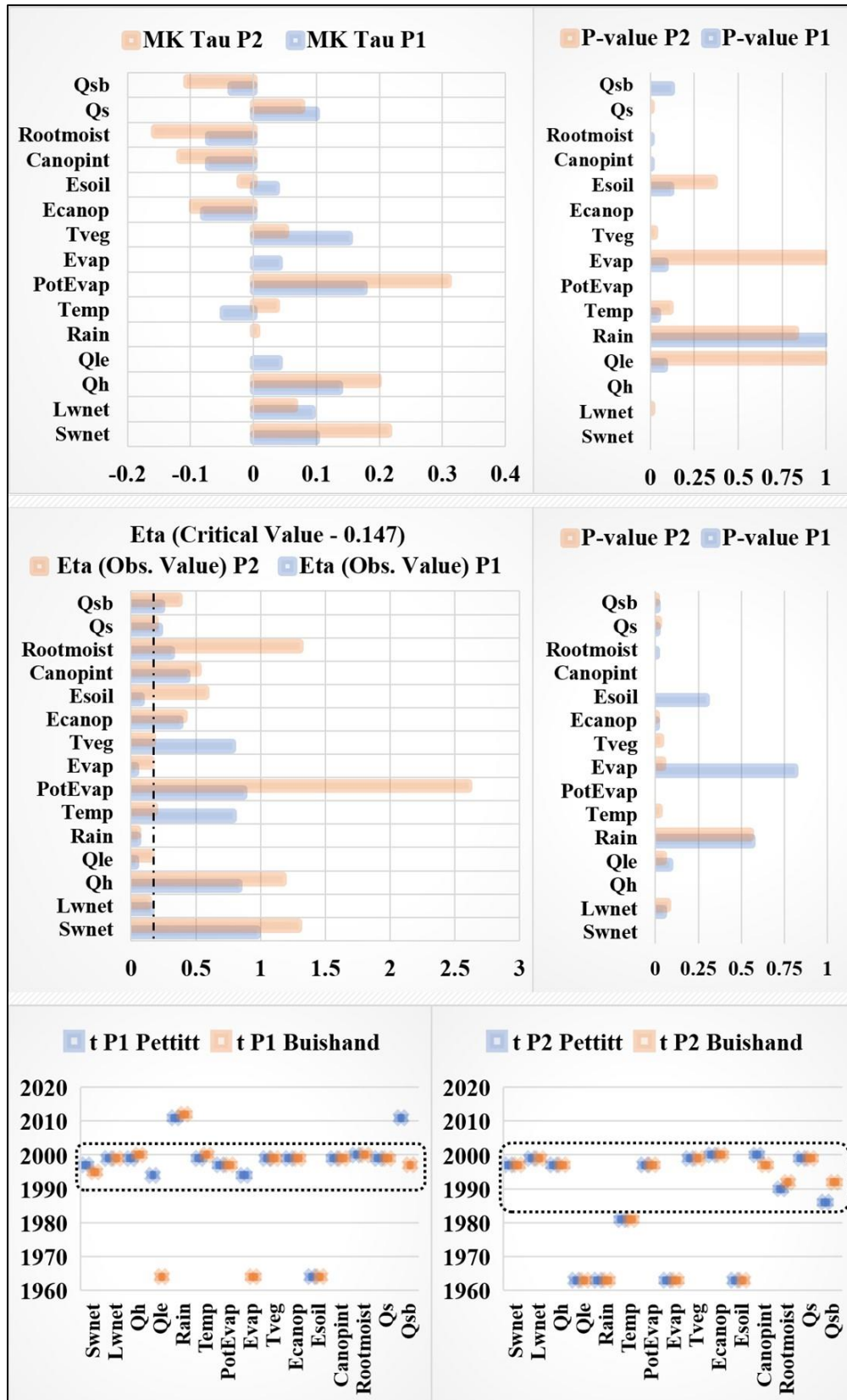
412 **Table 9** - Absolute and relative average variations of surface and subsurface runoff in SFB.

Variable	Average Variation - P1		Average Variation - P2	
	Absolute	Relative	Absolute	Relative
Qs	+ 64 mm/year	+ 400%	+37.6 mm/year	+ 4,700%
Qsb	- 162.4 mm/year	- 36%	- 88 mm/year	- 70%

413

414 Figure 4 shows in general how the trends of each variable from energy flow and water
 415 cycle behaved over the period evaluated. The results in Mann-Kendall test show that there were
 416 increases in heat and radiation flows across SFB, although on average the latent heat flow is
 417 stable at P2, in addition to stability in rainfall indexes. The KPSS test confirms such trends,
 418 showing that rainfall has a stationary behavior, both in P1 and in P2, over time, whereas for
 419 radiation and heat flows the critical value has been reaching, mainly for specific heat and short-
 420 wave radiation, showing a tendency towards non-stationarity throughout the series.

421 As a consequence of increase in radiation and heat flows, trends in potential and real
 422 evapotranspiration are positive, except for real evapotranspiration in P2, tending to stationarity.



425 **Figure 4** – Mann-Kendall, KPSS and Homogeneity tests (Pettitt and Buishand) for energy flow and water cycle
426 variables in SFB.

427 Although actual evapotranspiration did not keep up with the increase in potential, it was
428 positive due to the plant transpiration growth, as the water evaporation directly from plants'
429 canopies reduced, and evaporation directly from bare soils was stable. Even though in P2 the
430 KPSS test points out that there is no stationarity in the series, with a possible reduction.

431 The trends for the presence of moisture in plants' canopies and their root zones are
432 decreasing, ratified by non-stationarity in KPSS test. The reduction in humidity in these places is
433 probably due to the increase in evapotranspiration, but, mainly, to the rise in surface runoff,
434 which has a positive tendency, and to subsurface runoff reduction, which has a downward trend.
435 This shows less water infiltration in the soil, providing less moisture to plants' roots, and less
436 water containment by vegetation, reflected by less water maintenance in their canopies and
437 increase in water loss due to surface runoff.

438 All variables that showed a trend, positive or negative, with significant p-values, obtained
439 results in Pettitt and Buishand tests that showed a break in homogeneity mainly in the 1990s,
440 varying between 1995 and 2000 in P1, and between 1986 and 2000 in P2. The variables latent
441 heat, precipitation, evapotranspiration, direct water evaporation from bare soil and subsurface
442 runoff, whether in P1 and P2 or one of them, were those that obtained meanings that were more
443 distant from zero, being exactly those that showed a break in homogeneity in different years to
444 the rest of variables. This means that there was no break in their series, as the results in Mann-
445 Kendall and KPSS tests showed that the variables with most distant values of significance were
446 exactly those with no defined trend, that is, tending to stationarity.

447 **4.2 Spatiotemporal analyzes of land use and land cover**

448 Between 1985 and 2018 at SFB there was a reduction of 68,631 km² of native vegetation
449 formations, equivalent to 10.8% of the basin total area. From this reduction, 95.7% was caused
450 by agricultural activities (perennial and semi-perennial crops, planted forests and pastures), and
451 the remainder, 2,951 km² (4.3%), due to the advance of urban areas, mining and other uses
452 (Figure 5). The most degraded vegetation formations were savannas and grasslands, medium and
453 small sizes vegetations from Cerrado and Caatinga biomes and transition between them. The
454 third most affected were forests, of medium and large size, originating mainly in Atlantic Forest
455 biome, but also present in transition areas between these, Cerrado and Caatinga.

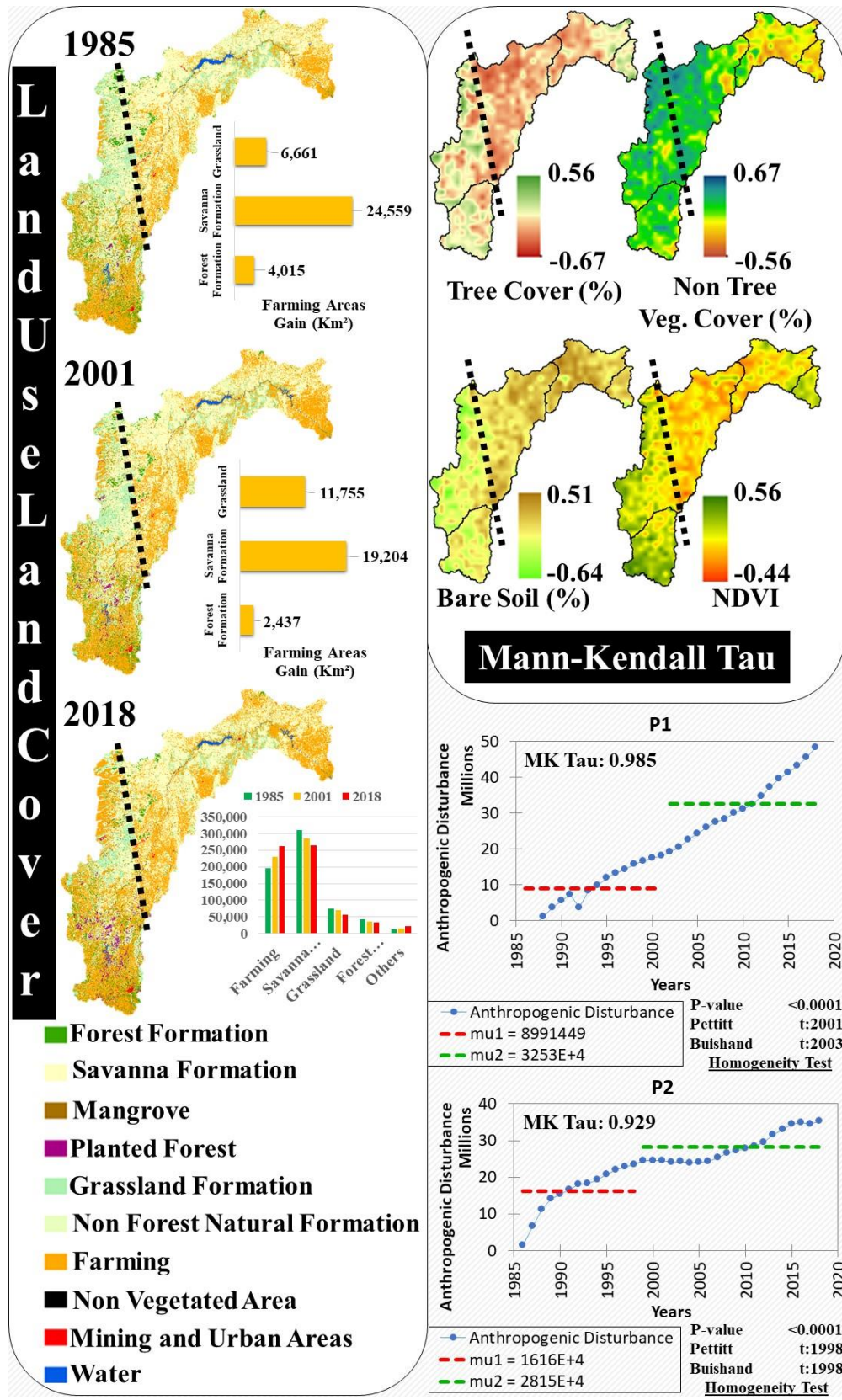


Figure 5 – Changes in land use and land cover in SFB and its effects on the presence of tree and non-tree vegetation cover and bare soil.

459 This reduction in native vegetation formations and their substitution by areas for
 460 agricultural use caused a fall in tree cover (Table 10), both in P1 and in P2. As for the non-tree
 461 cover, in P1 and P2 there was an increase, reflecting the pasture and crop expansion in detriment
 462 of forest and savanna areas, medium to large vegetation. The bare soil, at the same time, was
 463 reduced in P1, even with native vegetation degradation, due to territorial growth of agricultural
 464 cover. Although there were dynamics similar to P1 in P2, that is, the replacement of native
 465 vegetation with pastures and crops, there was a significant increase in bare soil, in contrast to
 466 what happened in P1.

467 **Table 10** - Changes in tree and non-tree vegetable coverings and bare soil in the SFB.

Tree Cover (%)			Non-Tree Cover (%)			Bare Soil (%)		
MK Statistics	P1	P2	MK Statistics	P1	P2	MK Statistics	P1	P2
Average	-0.06	-0.2	Average	0.2	0.1	Average	-0.13	0.1
Min.	-0.56	-0.58	Min.	-0.28	-0.44	Min.	-0.6	-0.58
Max.	0.56	0.56	Max.	0.67	0.67	Max.	0.51	0.51
Std. Dev.	0.21	0.18	Std. Dev.	0.18	0.23	Std. Dev.	0.21	0.17
MK Range (P1)	Area (%)		MK Range (P1)	Area (%)		MK Range (P1)	Area (%)	
-0.56 to 0	60		-0.28 to 0	15		-0.6 to 0	73	
0 to 0.56	40		0 to 0.67	85		0 to 0.51	27	
MK Range (P2)	Area (%)		MK Range (P2)	Area (%)		MK Range (P2)	Area (%)	
-0.58 to 0	87		-0.44 to 0	36		-0.58 to 0	30	
0 to 0.56	13		0 to 0.67	64		0 to 0.51	70	

468
 469 Between 1982 and 2014, in P1, tree cover reduced, on average, from 18.5% to 15%, and
 470 non-tree cover increased from 77.1% to 81.3%. Bare soil fell from 5.8% to 4%. In P2, tree cover
 471 dropped, on average, from 22% to 13.3%, and non-tree cover increased from 72.7% to 76.8%.
 472 Bare soil rose from 5.3% to 9.9%.

473 Concerning the NDVI (Table 11), even with drop in tree cover in P1, there was mostly an
 474 increase, which on average rose 0.06, from 0.50 to 0.56. In P2, in general, it remained stable,
 475 with a drop of 0.01, from 0.52 to 0.51, approximately half of the area falling and the remainder
 476 rising.

477 **Table 11** - Changes in NDVI in SFB.

MK Statistics	P1	MK Statistics	P2
Average	0.18	Average	0
Min.	-0.32	Min.	-0.35
Max.	0.56	Max.	0.56
Std. Dev.	0.17	Std. Dev.	0.13
MK Range (P1)	Area (%)	MK Range (P2)	Area (%)

-0.32 to 0	18	-0.35 to 0	57
0 to 0.56	82	0 to 0.56	43

478 The tests by Pettitt and Buishand (Figure 5), show that the break in homogeneity in
 479 historical series of land use and land cover occurred in the late 1990s for P1 and early 2000s for
 480 P2, very close to the results achieved for variables from the previous subtopic.

481 **4.3 Impacts and changes in São Francisco river' flow rate dynamics**

482 Although the drop in rainfall index in P1 was small, 5% between 1948 and 2019, the
 483 drought events of the last decade (2010-2019) affected the permanence flow curve of São
 484 Francisco river (Q_{95} and Q_{50}) (Figure 6). It is also noteworthy that these flows were influenced
 485 by the temporal behavior of rainfall, increasing when rainfall increases (between 1950 and 1989)
 486 and decreasing when rainfall drops (between 1990 and 2019).

487 Another relevant factor is the change in land cover caused by the expansion of activities
 488 and land uses, mainly linked to agriculture and livestock. Even though in P1 there was a fall in
 489 bare soils, this was accompanied by a reduction in tree vegetation cover and an increase in the
 490 non-tree vegetation cover, due exactly to increase in pastures and crops areas. This fact has
 491 implications for other variables related to energy flow and water cycle, such as the greater flow
 492 of radiation and, consequently, of heat, causing a greater evapotranspiration process, in addition
 493 to reduction in tree cover contribute to increase in surface runoff and reduction of water soil
 494 infiltration, reducing subsurface runoff and soil moisture in plants root zone.

495 Even with the reduction in rainfall during the 2000s and 2010s, surface runoff was greater
 496 than in previous decades, when there were similar or higher rainfall levels. This has an impact on
 497 the long-term flow rate of São Francisco river, given the precipitated water that drains
 498 superficially is reaching the watercourses faster due to reduction of friction caused by the
 499 replacement of the land cover. Thus, water soil infiltration reduced and caused less subsurface
 500 runoff, impairing the recharge of groundwater that supplies tributaries and the main river itself.
 501 This supply is even more important in drought periods.

502 In P2 (Figure 7), the situation is similar to P1, although there was a greater drop in tree
 503 cover and a greater increase in bare soil. The exception is the behavior of rainfall over the
 504 decades, which is not similar to that of flows rate (Figure 7). This occurs because in P2 the flow
 505 rate also follows the behavior of P1 rains, which are responsible for 65% of the water entering
 506 basin on average.

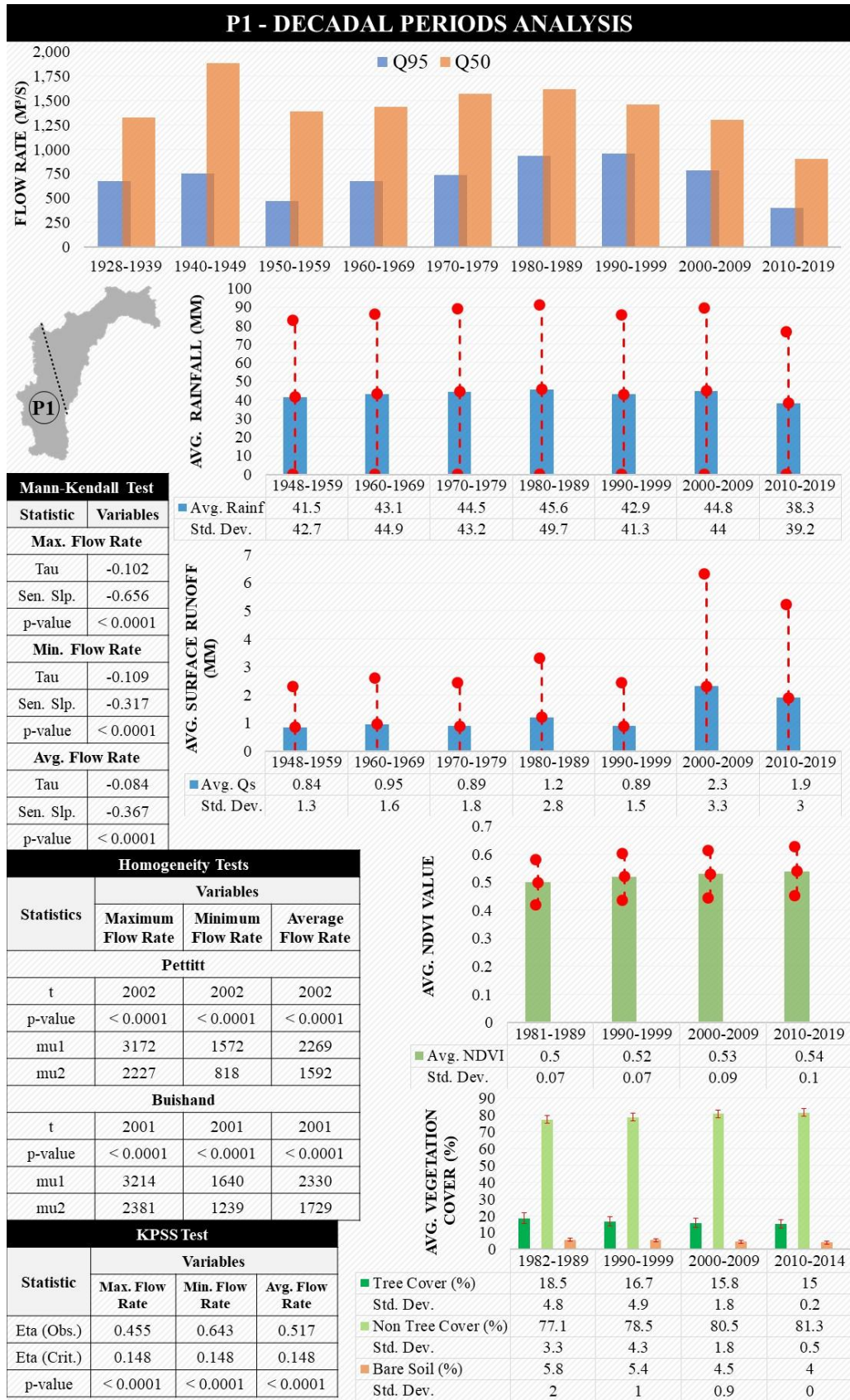


Figure 6 – Influence of rain dynamics and changes in land cover on the behavior of SFB flow rate in P1.

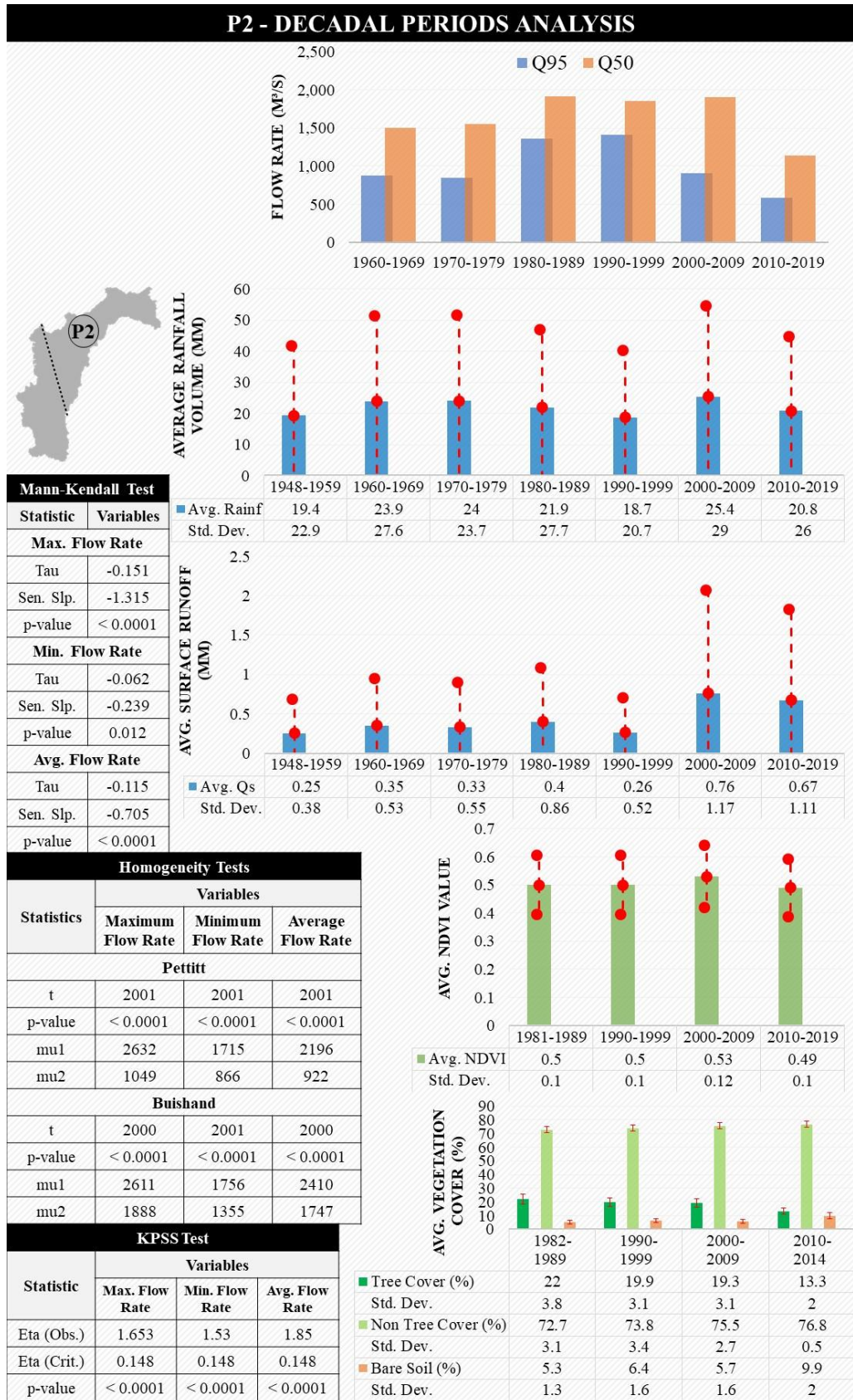


Figure 7 – Influence of rain dynamics and changes in land cover on the behavior of SFB flow rate in P2.

512 The impacts are even clearer when the statistical results referring to the maximum,
513 average and minimum flows rate are revealed, which show downward trends (MK) with values
514 of -0.102, -0.109 and -0.084 respectively, in P1 (Figure 6), and P2 (Figure 7) with values of -
515 0.151, -0.062 and -0.115. KPSS tests for all flows rate show that the critical levels have been
516 reached, reporting non-stationarity in the series. The tests by Pettitt and Buishand reveal that the
517 break in historical series homogeneity occurred in the early 2000s, in agreement with years
518 obtained for data on land use and land cover and very close to energy flow and water cycle
519 variables. This fact is a strong indication that changes in land use and land cover in SFB have
520 resulted in changes in the natural cycles of energy and water in basin.

521 It is also worth mentioning another factor that influenced the flows rate, which is the
522 construction of the Sobradinho dam, in the state of Bahia. Inaugurated in 1982, from then on the
523 dam contributed to regularization of the São Francisco flow rate. Between 1959 and 1980, in
524 rainy season, maximum and minimum flows rate reached values close to 4,600 and 2,800 m³/s,
525 respectively, and 1,200 and 1,100 m³/s, respectively, in drought period. From the 1980s to 2000s,
526 even with a certain increase in rainfall, maximum and minimum flows rate did not reach 3,600
527 and 2,400 m³/s, respectively, in rainy season, and exceeded 1,900 and 1,500 m³/s, respectively, in
528 drought period, showing a control of increase in flows rate when the rains occur with greater
529 frequency and intensity, and release when the drought occurs (Figure 8).

530 The flow rate regularization shown in the fluvioimetric station located in P2 does not
531 occur in the one located in P1, which reveals that there was a clear drop in the maximum and
532 minimum flows rate over the three periods evaluated, except for some similar values that occur
533 between the periods, notably in dry season. Comparing P2 to P1, the amplitude of maximum and
534 minimum flows rate between rainy and drought periods in 2001-2019, shows how the dams can
535 help to regulate water flow rate in watercourses and keep their availability even higher in
536 drought periods.

537 In P2, despite the reduction in rainfall between 2001 and 2019, there was an average drop
538 of 28% and 8% in maximum and minimum flows rate, respectively. In P1, the fall was 82% and
539 63%, respectively. This fact shows that without the construction of the dam, the situation in P2,
540 regarding water availability in São Francisco river, could have been more serious in drought
541 periods.

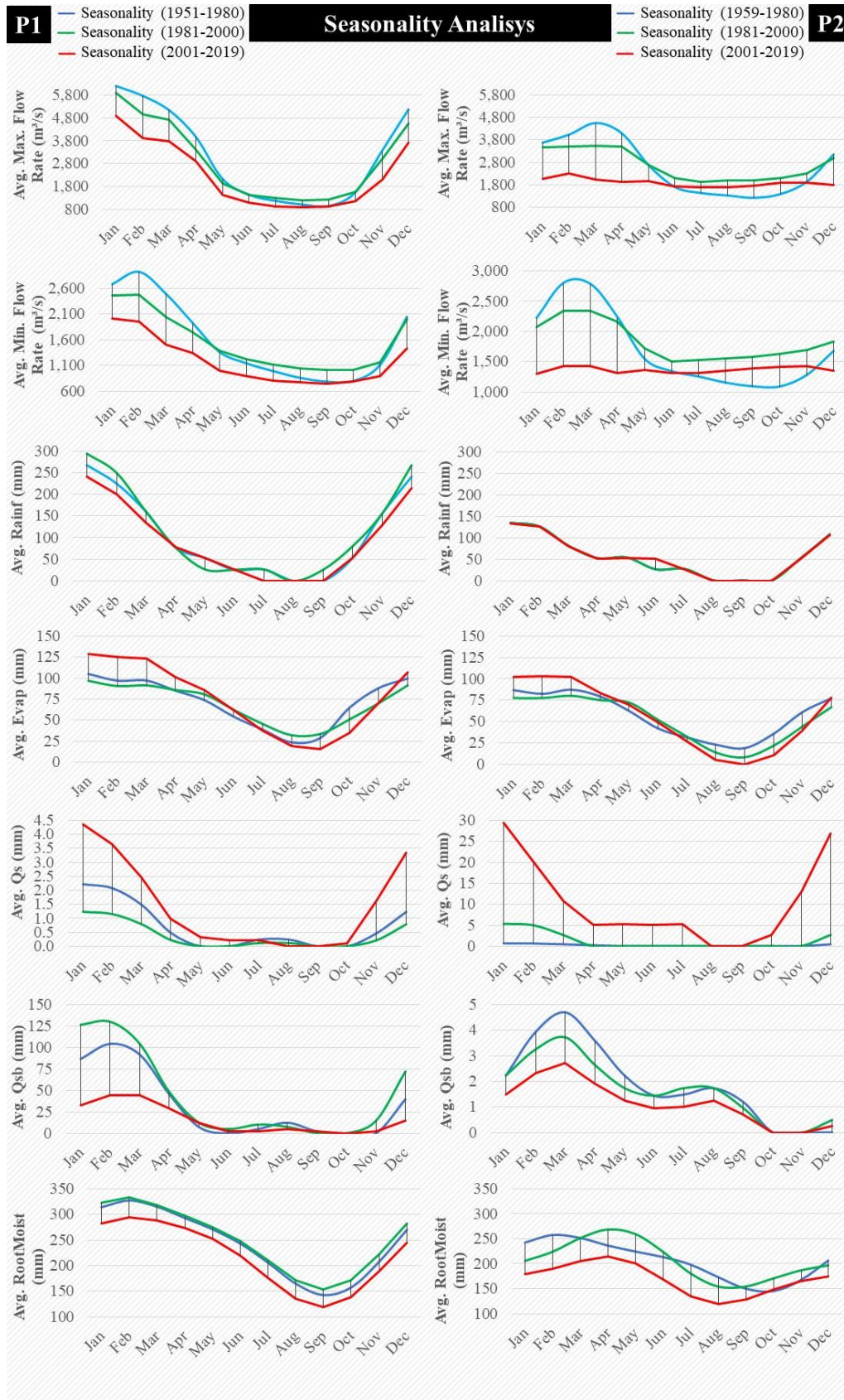


Figure 8 – Seasonal analysis of variables related to water cycle in the SFB.

544

545 In 2001-2019 period, in addition to a small reduction in rainfall in P1 and a stable
 546 situation in P2, there was also an increase in average evapotranspiration in rainy season and a
 547 reduction in drought in both areas (Table 12). There was an increase in average surface runoff
 548 practically throughout the year, notably in greatest rainfall period, and average subsurface runoff
 549 decreased, mainly in rainy season in P1. The presence of moisture in plants' root zone also
 550 dropped in the period 2001-2019, in both areas. The average reduction of 5% of rainfall in P1 is
 551 one of the factors related to the reduction of water present in basin, but the increase in
 552 evapotranspiration and surface runoff, caused by changes in land cover, had a greater impact on
 553 water maintenance.

554

Table 12 - Seasonal variation of water flow in SFB between 1951-1980 and 2001-2019.

Variable	Average Variation (P1)			
	Rainy Season		Dry Season	
	Absolute	Relative	Absolute	Relative
Rainf	-131 mm	-11%	-27 mm	-11%
Evap	+81 mm	+14%	-29 mm	-10%
Qs	+8.4 mm	+105%	+0.4 mm	+80%
Qsb	-201 mm	-55%	-2 mm	-7%
RootMoist	-152 mm	-9%	-146 mm	-12%
Variable	Average Variation (P2)			
	Rainy Season		Dry Season	
	Absolute	Relative	Absolute	Relative
Rainf	0 mm	0%	+26 mm	+16%
Evap	+33 mm	+7%	-47 mm	-19%
Qs	+102 mm	+3,792%	+24 mm	+2,380%
Qsb	-5 mm	-36%	-3 mm	-38%
RootMoist	-230 mm	-17%	-203 mm	-18%

555 The correlation (R) between the monthly data from January 1981 to December 2019 of
 556 NDVI with those of rain, evapotranspiration, root zone soil moisture of the plants, surface and
 557 subsurface runoff, shows, to a certain extent, the influence of vegetation maintaining humidity in
 558 basin.

559 Figure 9 shows how the NDVI has a higher correlation with rain, evapotranspiration and
 560 soil moisture in root zone. In other words, it shows how the seasonality of rainfall influences the
 561 seasonality of vegetation, with vegetation increasing its vigor in the rainy seasons and decreasing
 562 in the dry seasons, expect for some areas, probably influenced by local factors, such as relief,
 563 irrigation, among others.

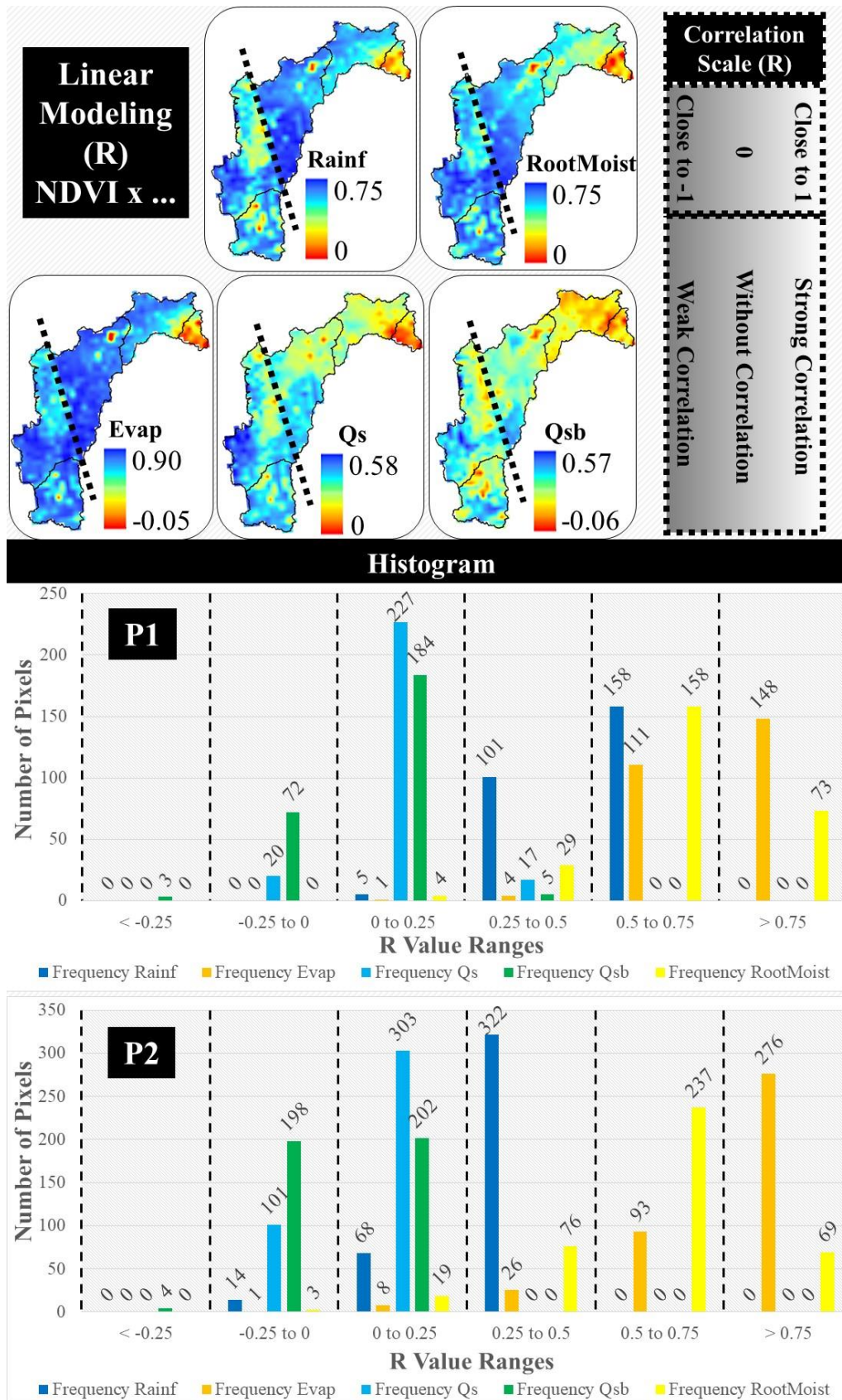


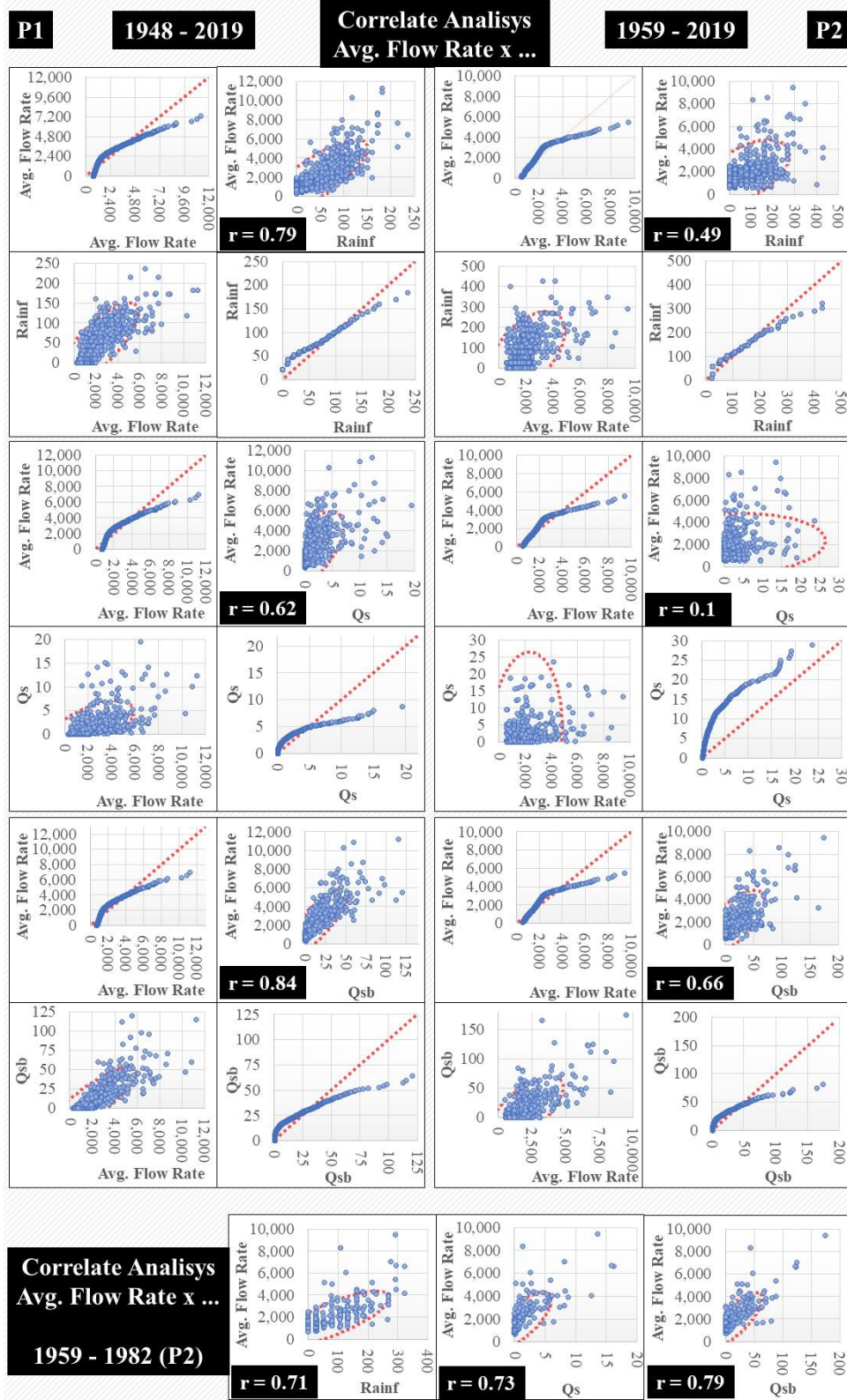
Figure 9 – Correlations between NDVI and water cycle variables in SFB.

566 The same occurs with soil moisture in root zone and with evapotranspiration, as in the
567 rainy seasons it tends to have a greater water accumulation in the soil, increasing its humidity,
568 and consequently a greater plant development, which also increases evapotranspiration
569 processes. In the dry seasons, the lower occurrence of rain decreases inlet of water into basin,
570 and with increase in energy flow (radiation and heat), it tends to increase potential
571 evapotranspiration, removing more water from the system by this process.

572 Although NDVI shows the vigor and health status of vegetation with some success, there
573 is some difficulty in defining its size, as there is no direct relationship between this and the
574 values of this index, depending a lot on the type of vegetation evaluated, in which biome and
575 climatic characteristics is located. For this reason, this index obtained lower correlations with
576 surface and subsurface runoff, which will vary according to the occurrence of precipitation. It
577 also depends on the relief and obstacles that favor or not water infiltration in soil and flow speed
578 on the surface, with plant sizes as important factors in this case. Land covers (bare soil, arboreal
579 and non-arboreal vegetation) were not used in this correlation because their information is of
580 annual frequency, and it is not possible to assess the seasonality of the process, which is
581 important in assessing the correlations, mainly due to the differences in the rainy and dry
582 seasons.

583 Correlating average monthly flow rate of the fluviometric stations located in P1 and P2,
584 with variables of rainfall, surface and subsurface runoff (Figure 10), it is clear their importance
585 in the flow rate dynamics over time. However, notably, as subsurface runoff is vital for
586 maintaining flow rate, especially in droughts. This shows how the recharge of groundwater is
587 essential during rainy periods, and this process has been hampered by changes in land cover
588 (Figure 11).

589 As seen earlier, Buishand and Pettitt tests show that the break in homogeneity for energy
590 flow, water cycle and land cover variables, occurred in the late 1990s and early 2000s, similar,
591 too, the result for these tests in the cases of flows rate in P1 and P2, which were between 2000
592 and 2002. Thus, concerning the pre and post-1990s periods, for the entire SFB, the average
593 reduction in rainfall volume was 2%, from 958.9 to 940.5 mm per year, down 18.4 mm. While
594 rainfall is stable, average evapotranspiration increased by 5% (+38.1 mm), surface runoff
595 increased by 225% (+36 mm) and water infiltration in the soil decreased by 52% (-92.5 mm)
596 (Figure 11).



597
598
599
600
601

Figure 10 – Correlations between average monthly flow rate with rainfall, surface and subsurface runoff data in SFB. Note: the construction of Sobradinho dam influenced the correlation values at the fluviometric station located in P2, due to flow rate regularization in São Francisco river, which significantly changed its behavior compared to other variables natural dynamics.

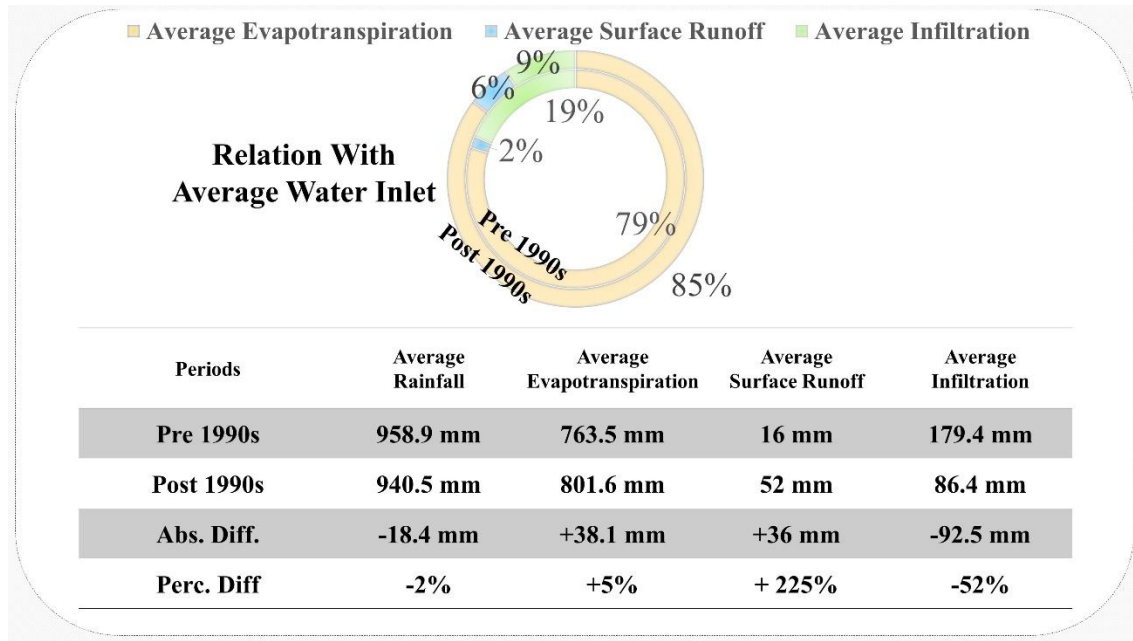


Figure 11 – Simplified water balance for the pre and post-1990s periods at SFB.

This means that in the period before the 1990s, from 100% of the water volume that entered the basin (precipitation), 79% returned to the atmosphere through evapotranspiration. In the current period, after the 1990s, this ratio is 85%. The loss through surface runoff was 2% and became 6%. In other words, there was a reduction in the water infiltration into the soil, which corresponded to 19% of the water volume, which entered the basin due to rains. This ratio has now dropped to 9% (Figure 11).

4 Conclusions

In this research, the following conclusions were reached:

- The variables related to energy flow and water cycle have undergone changes between 1948 and 2019, which contribute to evapotranspiration and surface runoff processes increase, and reduction of water infiltration in the soil, with drops in subsurface runoff and in humidity of the plants' root zone;
- The flow rate of São Francisco river has been impacted by such changes, since the water contribution of subsurface runoff has decreased in both P1 and P2, notably in the first, an area that represents 65% of the water entering SFB due to rain;
- The São Francisco river flow rate have been impacted mainly by the drop in the contribution of P1 in the maintenance of basin's water resources, notably by the reduction in

621 subsurface runoff of the last two decades, caused by the greater loss of water in surface runoff
622 and evapotranspiration;

623 • In summary, the very activities that depend on greater water maintenance in the basin are
624 those that promote water loss through surface runoff and evapotranspiration, reducing flow rates
625 of São Francisco river, by decreasing the recharge of aquifers and soil moisture.

626 **Acknowledgments, Samples, and Data**

627 This research was supported in part by a grant from the Coordenação de Aperfeiçoamento de
628 Pessoal de Nível Superior (CAPES) – Finance Code 001, belonging to the Education Ministry of
629 Brazil. The entire database was obtained from secondary sources, on the websites indicated in
630 subtopic 2.2, and duly referenced. The authors have no conflicts of interest to declare.

631 **References**

- 632 Ala-aho, P., Soulsby, C., Wang, H., & Tetzlaff, D. (2017). Integrated surface-subsurface model
633 to investigate the role of groundwater in headwater catchment runoff generation: A
634 minimalist approach to parameterisation. *Journal of Hydrology*, *547*, 664–677.
635 <https://doi.org/10.1016/j.jhydrol.2017.02.023>
- 636 Alcoforado de Moraes, M. M. G., Biewald, A., Carneiro, A. C. G., Souza da Silva, G. N., Popp,
637 A., & Lotze-Campen, H. (2018). The impact of global change on economic values of water
638 for Public Irrigation Schemes at the São Francisco River Basin in Brazil. *Regional*
639 *Environmental Change*, *18*(7), 1943–1955. <https://doi.org/10.1007/s10113-018-1291-0>
- 640 Barber, C., Lamontagne, J. R., & Vogel, R. M. (2020). Improved estimators of correlation and R^2
641 for skewed hydrologic data. *Hydrological Sciences Journal*, *65*(1), 87–101.
642 <https://doi.org/10.1080/02626667.2019.1686639>
- 643 Beaudoin, H., & Rodell, M. (2019). GLDAS Noah Land Surface Model L4 monthly 0.25 x 0.25
644 degree V2.0, Greenbelt, Maryland, USA, Goddard Earth Sciences Data and Information
645 Services Center (GES DISC). <https://doi.org/10.5067/9SQ1B3ZXP2C5>
- 646 Bezerra, B. G., Silva, L. L., Santos e Silva, C. M., & de Carvalho, G. G. (2019). Changes of
647 precipitation extremes indices in São Francisco River Basin, Brazil from 1947 to 2012.
648 *Theoretical and Applied Climatology*, *135*(1–2), 565–576. [https://doi.org/10.1007/s00704-](https://doi.org/10.1007/s00704-018-2396-6)
649 [018-2396-6](https://doi.org/10.1007/s00704-018-2396-6)
- 650 Bickici Arıkan, B., & Kahya, E. (2019). Homogeneity revisited: analysis of updated precipitation
651 series in Turkey. *Theoretical and Applied Climatology*, *135*(1–2), 211–220.
652 <https://doi.org/10.1007/s00704-018-2368-x>
- 653 Buishand, T. A. (1982). Some methods for testing the homogeneity of rainfall records. *Journal*
654 *of Hydrology*, *58*(1–2), 11–27. [https://doi.org/10.1016/0022-1694\(82\)90066-X](https://doi.org/10.1016/0022-1694(82)90066-X)
- 655 Correia, R. C., Araújo, J. L. P., & Cavalcanti, E. de B. (2001). A fruticultura como vetor de
656 desenvolvimento: o caso dos municípios de Petrolina (PE) e Juazeiro (BA). - Portal
657 Embrapa. In R. C. (Embrapa S.-C. Correia & J. L. P. (Embrapa S.-C. Araujo (Eds.),
658 *CONGRESSO BRASILEIRO DE ECONOMIA E SOCIOLOGIA RURAL*. (39th ed., p. 8).

- 659 Recife, Brasil: SOBER/ESALQ/EMBRAPA/UFPE/URFPE. Retrieved from
660 [https://www.embrapa.br/busca-de-publicacoes/-/publicacao/134327/a-fruticultura-como-
vetor-de-desenvolvimento-o-caso-dos-municipios-de-petrolina-pe-e-juazeiro-ba](https://www.embrapa.br/busca-de-publicacoes/-/publicacao/134327/a-fruticultura-como-
661 vetor-de-desenvolvimento-o-caso-dos-municipios-de-petrolina-pe-e-juazeiro-ba)
- 662 Creech, C. T., Siqueira, R. B., Selegean, J. P., & Miller, C. (2015). Anthropogenic impacts to the
663 sediment budget of São Francisco River navigation channel using SWAT. *International
664 Journal of Agricultural and Biological Engineering*, 8(3), 1–20.
665 <https://doi.org/10.3965/j.ijabe.20150803.1372>
- 666 Das, P., Behera, M. D., Patidar, N., Sahoo, B., Tripathi, P., Behera, P. R., et al. (2018). Impact of
667 LULC change on the runoff, base flow and evapotranspiration dynamics in eastern Indian
668 river basins during 1985–2005 using variable infiltration capacity approach. *Journal of
669 Earth System Science*, 127(2), 19. <https://doi.org/10.1007/s12040-018-0921-8>
- 670 Didan, K., & Barreto, A. (2016). NASA MEaSURES Vegetation Index and Phenology (VIP)
671 Vegetation Indices Monthly Global 0.05Deg CMG [Data set].
672 <https://doi.org/10.5067/MEaSURES/VIP/VIP30.004>
- 673 Eastman, J. R. (2016). Terrset: Geospatial Monitoring and Modeling System Manual. Retrieved
674 September 10, 2020, from [https://clarklabs.org/wp-content/uploads/2016/10/Terrset-
Manual.pdf](https://clarklabs.org/wp-content/uploads/2016/10/Terrset-
675 Manual.pdf)
- 676 Hansen, M., & Song, X. P. (2018). Vegetation Continuous Fields (VCF) Yearly Global 0.05 Deg
677 [Data set]. <https://doi.org/10.5067/MEaSURES/VCF/VCF5KYR.001>
- 678 Hirsch, R. M., & Slack, J. R. (1984). A Nonparametric Trend Test for Seasonal Data With Serial
679 Dependence. *Water Resources Research*, 20(6), 727–732.
680 <https://doi.org/10.1029/WR020i006p00727>
- 681 Hirsch, R. M., Slack, J. R., & Smith, R. A. (1982). Techniques of trend analysis for monthly
682 water quality data. *Water Resources Research*, 18(1), 107–121.
683 <https://doi.org/10.1029/WR018i001p00107>
- 684 Jiang, S., Wei, L., Ren, L., Xu, C. Y., Zhong, F., Wang, M., et al. (2021). Utility of integrated
685 IMERG precipitation and GLEAM potential evapotranspiration products for drought
686 monitoring over mainland China. *Atmospheric Research*, 247, 105141.
687 <https://doi.org/10.1016/j.atmosres.2020.105141>
- 688 de Jong, P., Tanajura, C. A. S., Sánchez, A. S., Dargaville, R., Kiperstok, A., & Torres, E. A.
689 (2018). Hydroelectric production from Brazil's São Francisco River could cease due to
690 climate change and inter-annual variability. *Science of the Total Environment*, 634, 1540–
691 1553. <https://doi.org/10.1016/j.scitotenv.2018.03.256>
- 692 Kendall, M. (1975). *Multivariate analysis*. London: Charles Griffim & Company Ltd.
- 693 Koch, H., Biewald, A., Liersch, S., Azevedo, J. R. G. de, Silva, G. N. S. da, Kölling, K., et al.
694 (2015). Scenarios of climate and land-use change, water demand and water availability for
695 the São Francisco River basin. *Revista Brasileira de Ciências Ambientais (Online)*, (36),
696 96–114. <https://doi.org/10.5327/z2176-947820151007>
- 697 Kwiatkowski, D., Phillips, P. C. B., Schmidt, P., & Shin, Y. (1992). Testing the null hypothesis
698 of stationarity against the alternative of a unit root. How sure are we that economic time
699 series have a unit root? *Journal of Econometrics*, 54(1–3), 159–178.

- 700 [https://doi.org/10.1016/0304-4076\(92\)90104-Y](https://doi.org/10.1016/0304-4076(92)90104-Y)
- 701 Lindsey, R. (2009). *Climate and Earth's Energy Budget*. Retrieved from
702 <https://earthobservatory.nasa.gov/features/EnergyBalance>
- 703 Mann, H. B. (1945). Nonparametric Tests Against Trend. *Econometrica*, 13(3), 245.
704 <https://doi.org/10.2307/1907187>
- 705 Mokhtari, A., Noory, H., & Vazifedoust, M. (2018). Performance of Different Surface Incoming
706 Solar Radiation Models and Their Impacts on Reference Evapotranspiration. *Water*
707 *Resources Management*, 32(9), 3053–3070. <https://doi.org/10.1007/s11269-018-1974-9>
- 708 Pereira, S. B., Pruski, F. F., Da Silva, D. D., & Ramos, M. M. (2007). Study of the hydrological
709 behavior of São Francisco River and its main tributaries. *Revista Brasileira de Engenharia*
710 *Agrícola e Ambiental*, 11(6), 615–622. <https://doi.org/10.1590/S1415-43662007000600010>
- 711 Pettitt, A. N. (1979). A Non-Parametric Approach to the Change-Point Problem. *Applied*
712 *Statistics*, 28(2), 126. <https://doi.org/10.2307/2346729>
- 713 Pruski, F. F., Pereira, S. B., Novaes, L. F. de, Silva, D. D. da, & Ramos, M. M. (2004). Specific
714 yield discharge and mean precipitation in São Francisco Basin. *Revista Brasileira de*
715 *Engenharia Agrícola e Ambiental*, 8(2–3), 247–253. <https://doi.org/10.1590/s1415-43662004000200013>
- 717 Rodell, M., Houser, P. R., Jambor, U., Gottschalck, J., Mitchell, K., Meng, C. J., et al. (2004).
718 The Global Land Data Assimilation System. *Bulletin of the American Meteorological*
719 *Society*, 85(3), 381–394. <https://doi.org/10.1175/BAMS-85-3-381>
- 720 Rougé, C., Ge, Y., & Cai, X. (2013). Detecting gradual and abrupt changes in hydrological
721 records. *Advances in Water Resources*, 53, 33–44.
722 <https://doi.org/10.1016/j.advwatres.2012.09.008>
- 723 Serinaldi, F., & Kilsby, C. G. (2015). Stationarity is undead: Uncertainty dominates the
724 distribution of extremes. *Advances in Water Resources*, 77, 17–36.
725 <https://doi.org/10.1016/j.advwatres.2014.12.013>
- 726 Serinaldi, F., Kilsby, C. G., & Lombardo, F. (2018). Untenable nonstationarity: An assessment
727 of the fitness for purpose of trend tests in hydrology. *Advances in Water Resources*, 111,
728 132–155. <https://doi.org/10.1016/j.advwatres.2017.10.015>
- 729 Seyoum, W. M., & Milewski, A. M. (2017). Improved methods for estimating local terrestrial
730 water dynamics from GRACE in the Northern High Plains. *Advances in Water Resources*,
731 110, 279–290. <https://doi.org/10.1016/j.advwatres.2017.10.021>
- 732 Souza, C. M., Z. Shimbo, J., Rosa, M. R., Parente, L. L., A. Alencar, A., Rudorff, B. F. T., et al.
733 (2020). Reconstructing Three Decades of Land Use and Land Cover Changes in Brazilian
734 Biomes with Landsat Archive and Earth Engine. *Remote Sensing*, 12(17), 2735.
735 <https://doi.org/10.3390/rs12172735>
- 736 Sun, T., Ferreira, V., He, X., & Andam-Akorful, S. (2016). Water Availability of São Francisco
737 River Basin Based on a Space-Borne Geodetic Sensor. *Water*, 8(5), 213.
738 <https://doi.org/10.3390/w8050213>
- 739 Torres, M. D. O., Maneta, M., Howitt, R., Vosti, S. A., Wallender, W. W., Bassoi, L. H., &

- 740 Rodrigues, L. N. (2012). Economic impacts of regional water scarcity in the São Francisco
741 river Basin, Brazil: An application of a linked hydro-economic model. *Environment and*
742 *Development Economics*, 17(2), 227–248. <https://doi.org/10.1017/S1355770X11000362>
- 743 Umair, M., Kim, D., & Choi, M. (2019). Impacts of land use/land cover on runoff and energy
744 budgets in an East Asia ecosystem from remotely sensed data in a community land model.
745 *Science of The Total Environment*, 684, 641–656.
746 <https://doi.org/10.1016/j.scitotenv.2019.05.244>
- 747 Yan, G., Jiao, Z. H., Wang, T., & Mu, X. (2020). Modeling surface longwave radiation over
748 high-relief terrain. *Remote Sensing of Environment*, 237, 111556.
749 <https://doi.org/10.1016/j.rse.2019.111556>
- 750 Yang, F., Lu, H., Yang, K., He, J., Wang, W., Wright, J. S., et al. (2017). Evaluation of multiple
751 forcing data sets for precipitation and shortwave radiation over major land areas of China.
752 *Hydrology and Earth System Sciences*, 21(11), 5805–5821. [https://doi.org/10.5194/hess-21-](https://doi.org/10.5194/hess-21-5805-2017)
753 [5805-2017](https://doi.org/10.5194/hess-21-5805-2017)
- 754 Yin, L., Feng, X., Fu, B., Chen, Y., Wang, X., & Tao, F. (2020). Irrigation water consumption of
755 irrigated cropland and its dominant factor in China from 1982 to 2015. *Advances in Water*
756 *Resources*, 143, 103661. <https://doi.org/10.1016/j.advwatres.2020.103661>
- 757 Yozgatligil, C., & Yazici, C. (2016). Comparison of homogeneity tests for temperature using a
758 simulation study. *International Journal of Climatology*, 36(1), 62–81.
759 <https://doi.org/10.1002/joc.4329>
- 760 Yuan, R. Q., Chang, L. L., Gupta, H., & Niu, G. Y. (2019). Climatic forcing for recent
761 significant terrestrial drying and wetting. *Advances in Water Resources*, 133, 103425.
762 <https://doi.org/10.1016/j.advwatres.2019.103425>
- 763